Research Square

Preprints are preliminary reports that have not undergone peer review.
They should not be considered conclusive, used to inform clinical practice,
or referenced by the media as validated information.

The Warburg Effect Hallmark in Nasopharyngeal Carcinoma: Stage-Specific Up-Regulation of LDHA, GAPDH, CS, CYC, MRPL3, and TIMMDC1 Drives a Hybrid Glycolysis/OXPHOS Profile during Regional Progression

Maria-Jose Oliach

oliach.mj@gmail.com

Independent Researcher. Tarragona. Spain

Antonio R. Romeu

University Rovira i Virgili. Tarragona. Spain

Research Article

Keywords: Nasopharyngeal Carcinoma, Warburg Effect, Up-regulation, Core Metabolic Signature, Hybrid Phenotype, limma R package, Citrate Synthase

Posted Date: July 3rd, 2026

DOI: https://doi.org/10.21203/rs.3.rs-10225258/v1

License: This work is licensed under a Creative Commons Attribution 4.0 International License.
Read Full License

Additional Declarations: The authors declare no competing interests.

The Warburg Effect Hallmark in Nasopharyngeal Carcinoma: Stage-Specific Up-Regulation of LDHA, GAPDH, CS, CYC, MRPL3, and TIMMDC1 Drives a Hybrid Glycolysis/OXPHOS Profile during Regional Progression

Maria-Jose Oliach[1], Antonio R. Romeu[2,3,]

1. Independent Researcher. Tarragona. Spain
2. University Rovira i Virgili. Tarragona. Spain.
3. Corresponding author. Email: antonioramon.romeu@iubilo.urv.cat

Abstract

Background: Nasopharyngeal carcinoma (NPC) is an aggressive epithelial malignancy with distinct clinical dynamics across its developmental stages. While metabolic reprogramming is a recognized hallmark of cancer, the stage-specific activation of aerobic glycolysis—the Warburg effect—and its exact molecular indicators during NPC progression remain to be fully mapped. This study evaluates the precise transcriptional trajectories of key metabolic players to identify stage-dependent bioenergetic checkpoints.

Methods: Using transcriptomic data from the NCBI GEO database (dataset GDS3341/GSE12452, platform GPL570), we performed a differential expression analysis using the R package 'limma'. We evaluated a targeted panel of 155 genes representing key metabolic pathways of the Warburg effect across five developmental stages: T1N0, T1N1, T2N1, T2N2, and T3N2.

Results: The analysis revealed a highly coordinated metabolic shift concentrated in advanced regional stages (T2N1, T2N2, and T3N2). We identified a metabolic signature characterized by the significant stage-specific up-regulation of six core genes: LDHA, GAPDH, CS, CYC, MRPL3, and TIMMDC1 Beyond this core panel, twelve additional metabolic genes exhibited stage-specific variations. Glycolytic acceleration and microenvironment adaptation were further evidenced by the up-regulation of TPI1 and the lactate transporter SLC16A1 (MCT1). Concurrently, specific chaperones for Complexes I, II, III, and V were up-regulated. The cytochrome c oxidase assembly factor COA8 in T2N1 and T3N2 stages was the unique down-regulation. However, the lack of significance in T1N1 does not weaken the model; rather, it underscores that the hybrid metabolic phenotype is a specialized hallmark of advanced, high-risk regional NPC progression.

Conclusions: NPC progression is driven by a stage-dependent manifestation of the Warburg effect hallmark. Advanced-stage tumor cells establish an active hybrid glycolysis/oxidative phosphorylation (OXPHOS) phenotype or state characterized by the coordinated up-regulation of LDHA, GAPDH, CS, CYC, MRPL3, and TIMMDC1.

Keywords: Nasopharyngeal Carcinoma; Warburg Effect; Up-regulation; Core Metabolic Signature; Hybrid Phenotype; limma R package, Citrate Synthase.

Introduction

Nasopharyngeal carcinoma (NPC) is a malignant epithelial tumor of the nasopharynx [1,2] that exhibits a distinctive geographic distribution and a complex etiology driven by genetic susceptibility, environmental factors, and Epstein-Barr virus (EBV) infection [3,4]. Large proportion of NPC patients are diagnosed at advanced tumor (T) and nodal (N) stages [5,6]. Over the last decades, transcriptomic profiling of microarrays has significantly enhanced our understanding of the molecular alterations driving NPC, offering valuable tools to identify diagnostic biomarkers and potential therapeutic targets [7-9]. However, analyzing how these altered cellular pathways interact and evolve throughout clinical staging remains a fundamental challenge in understanding NPC progression.

Over the past two decades, metabolic reprogramming has transitioned from being considered a mere epiphenomenon of oncogenesis to a well-established core hallmark of cancer [10]. Neoplastic cells universally alter their metabolic infrastructure to sustain the bioenergetic, biosynthetic, and redox demands dictated by rapid proliferation and survival under microenvironmental stress [11]. The most classical iteration of this metabolic rewiring is the "Warburg effect, or aerobic glycolysis, wherein cancer cells preferentially ferment glucose into lactate even in the presence of ambient oxygen [12].

Our previous research [13,14] established a structured bioinformatic framework to identify robust, stage-independent molecular markers in NPC using public microarray datasets. In our first study, we demonstrated that highly expressed genes can effectively stratify NPC progression, highlighting a prominent dysregulation of the transferrin receptor (TFRC) as a key clinical hallmark. Building upon this finding, our second study shifted focus toward cellular protection mechanisms on chromosome 6p12. We discovered a coordinated, stage-independent downregulation of the glutathione S-transferase alpha cluster (GSTA1 and GSTA3). This severe impairment of the cellular detoxification machinery suggested that NPC cells undergo a chronic state of oxidative stress and metabolic rewiring that remains active from early clinical stages to advanced metastatic disease.

This third study represents a logical next step along this scientific thread, moving from iron homeostasis and antioxidant failure directly into the core of NPC energy metabolism: the Warburg effect. Our preliminary screening of NPC data revealed a persistent, stage-independent over-expression of the critical mitochondrial enzyme citrate synthase (CS). This unexpected hyperactivation of key step in the tricarboxylic acid (TCA) cycle suggests that NPC mitochondria are not dysfunctional or dormant, but rather reprogrammed to actively divert carbon resources toward biomass synthesis and lipid production.

Consequently, the objective of this study is to perform a comprehensive, stage-by-stage bioinformatic characterization of the major metabolic pathways—glycolysis, the TCA cycle, and the mitochondrial respiratory chain (OXPHOS)—in NPC using a fine-staged clinical model. By examining a curated panel of hallmark metabolic genes (including transport systems like GLUT1 and MCT4, and regulatory nodes like PDK1, FASN, and G6PD), we aim to clarify how glucose oxidation is decoupled from mitochondrial respiration in this tumor. This study provides a unified metabolic model that connects our previous findings on iron uptake and antioxidant depletion with the broader landscape of energetic reprogramming, establishing a solid foundation to understand how metabolic hallmarks sustain the structural progression of nasopharyngeal carcinoma. We utilized the GDS3341 dataset [7-9] from the National Center for Biotechnology Information (NCBI) Gene Expression Omnibus (GEO) database [15,16].

Methodology

Nasopharyngeal carcinoma transcriptomic expression data were sourced from the public NCBI Gene Expression Omnibus (GEO) repository under dataset accession GDS3341 (series GSE12452). The dataset comprises high-throughput gene expression profiles generated using the Affymetrix Human Genome U133 Plus 2.0 Array platform (GPL570), encompassing progressive clinical stages of NPC along with non-tumor control tissues. Raw data processing, background correction, and intra-array quantile normalization were executed via the Robust Multi-array Average (RMA) algorithm. To ensure rigorous probe-to-gene mapping, multi-probe identification numbers for individual loci were collapsed to official HUGO Gene Nomenclature Committee (HGNC) gene symbols by selecting the specific probe set demonstrating the maximum average expression baseline across all samples.

Differential expression analysis was performed utilizing the linear modeling and empirical Bayes moderation framework within the limma package in R. To determine the transcriptional dynamics of metabolic reprogramming, a subset of 155 targeted genes representing core glycolytic checkpoints, the tricarboxylic acid (TCA) cycle, and mitochondrial oxidative phosphorylation (OXPHOS) pathways was systematically extracted (Table 1S). Contrast matrices were constructed to evaluate pairwise differential expression by comparing individual advanced clinical stages -specifically T2N1, T2N2, and T3N2- against healthy non-tumor control baselines. Raw P-values were adjusted for multiple testing using the Benjamini-Hochberg False Discovery Rate (FDR) correction procedure (adj.P.Val). Transcriptional alterations were considered statistically roburobust and significant when achieving an adjusted (P-value < 0.05) accompanied by an empirical Bayes log-odds score (B-statistic) strictly greater than 0 ($B > 0$).

Results and Discussion

Using the NCBI GEO dataset GDS3341 / GSE12452. Differential expression analysis via the limma package revealed that regional nodal progression is governed by a highly selective transcriptional signature rather than a generalized metabolic deregulation. Specifically, a restricted subset of six genes—comprising the glycolytic enzymes *LDHA* and *GAPDH*, the tricarboxylic acid cycle enzyme CS, the electron transport chain component CYC, and the mitochondrial biogenesis and assembly factors *MRPL3* and *TIMMDC1*—demonstrated a robust, consistent upregulation exclusive to the advanced lymph node involvement stages (T1N2, T2N2, and T3N2) (Table 1 and Figure 1).

Beyond this core panel, twelve additional metabolic genes exhibited stage-specific variations. Glycolytic acceleration and microenvironment adaptation were further evidenced by the up-regulation of TPI1 and the lactate transporter SLC16A1 (MCT1). Concurrently, specific chaperones for Complexes I, II, III, and V were up-regulated. The cytochrome c oxidase assembly factor COA8 in T2N1 and T3N2 stages was the unique down-regulation (Table 2).

The dual upregulation of both critical glycolytic checkpoints and key mitochondrial elements (Table 1) suggests a precise oncogenic coordination. Instead of a unilateral metabolic shift, aggressive NPC cells in advanced *N* stages seem to establish a hybrid metabolic phenotype, co-activating specific rate-limiting nodes in both the cytosol and mitochondria to sustain the bioenergetic and biosynthetic demands of regional metastasis. The simultaneous upregulation of the glycolytic machinery (LDHA and GAPDH) along with core mitochondrial components (CS and CYC) highlights the establishment of a hybrid glycolysis/OXPHOS metabolic phenotype in advanced regional nodal stages (N2). Biochemically, this co-activation solves a critical bioenergetic and

biosynthetic dilemma inherent to metastasizing cells. While LDHA induction accelerates ATP production via high-flux glycolysis to meet immediate energetic demands and promotes microenvironmental acidification via lactate, the concurrent upregulation of Citrate Synthase (CS) does not imply a conventional alignment toward complete glucose oxidation. Instead, CS serves as the fundamental gatekeeper for mitochondrial macromolecular synthesis. CS upregulation should be interpreted as a molecular strategy to enhance the tumour energy supply or tumour fuel to growth and proliferation. Depending on the cancer type, CS exhibits both oncogenic and tumour-suppressing characteristics [17-24]. In cancers like prostate, ovarian, and pancreatic CS expression is upregulated [47-49]. Our results are consistent with those described by L. Guo *et al.* (2024) [24] that directly link the upregulation of CS with the progression and malignancy of NPC. By maintaining high CS expression, NPC cells become resistant to oxidative stress induced by drugs such as erastin [24]. Excess CS protein within mitochondria directly stimulates proliferation, cell migration, and tissue invasion of nasopharyngeal carcinoma [24]. In summary, citrate synthase (CS) overexpression in NPC can be considered a cellular resistance mechanism that promotes tumour dissemination, positioning CS inhibition as a promising NPC therapeutic strategy.

Data from limma results (Table 1) reveal that the six critical enzymatic and structural nodes are aggressively driven into the high-significance. This successfully refutes the possibility of an experimental batch effect or artifacts from microarray normalization. Instead, it mathematically underscores that advanced regional metastasis in NPC does not stem from a chaotic, global deregulation of the cellular transcriptome. Rather, it relies on a highly selective, targeted activation of precise cytosolic glycolytic checkpoints and key mitochondrial biogenesis and respiratory chain elements, establishing the hybrid metabolic phenotype required for advanced nodal dissemination (N1 to N2).

Notably, the contrast evaluating the early regional nodal involvement stage, T1N1 (n = 10), did not yield statistically significant differential expression for any of the 155 metabolic genes analyzed (Figure 1B). While this apparent lack of transcriptional divergence might initially seem unexpected for an intermediate clinical phenotype, it can be explained by a combination of statistical and biological factors. Statistically, a sample size of (n = 10) inherently limits the statistical power of the limma empirical Bayes framework when correcting for multiple testing via the False Discovery Rate (FDR). In heterogenous clinical cohorts, subtle biological variations among individual patients within early-stage subcategories can increase intra-group variance, thereby suppressing the t-statistics and preventing true biological signals from achieving adjusted P-values below the stringent (0.05) threshold. Biologically, this finding strongly suggests that low-volume, early-stage lymph node metastasis (N1) in the context of a small primary tumor (T1) represents a transitional, metabolic-neutral state. The metabolic rewiring toward a hybrid glycolysis/OXPHOS phenotype appears not to be a linear process that scales gradually with tumor progression. Instead, our data demonstrate that this metabolic switch acts as a threshold-dependent event. The robust transcriptional activation of genes such as LDHA, GAPDH, and CS is strictly required only when the tumor undergoes critical regional expansion and high-burden nodal colonization, as clearly evidenced by the abrupt and definitive significance observed in the subsequent advanced stages T2N1, T2N2 and 3N2. Therefore, the lack of significance in T1N1 does not weaken the model; rather, it underscores that the hybrid metabolic phenotype is a specialized hallmark of advanced, high-risk regional progression.

Conclusions

Based on the differential expression analysis of Warburg effect-associated genes across different stages of nasopharyngeal carcinoma (NPC), the following main conclusions can be drawn:

- Stagewise Metabolic Reprogramming. NPC progression is characterized by a dynamic and coordinated metabolic shift that intensifies in advanced stages (T2N1, T2N2, and T3N2), confirming that the Warburg effect acts as a key driver of advanced tumor development rather than a static baseline feature.
- Core Six-Gene Metabolic Signature. The robust and significant dysregulation of the core six genes (LDHA, MRPL3, TIMMDC1, CYC, CS, and GAPDH) establishes a reliable molecular signature of metabolic adaptation, pinpointing the exact transition phases where energy production shifts heavily toward alternative pathways.
- Enhanced Glycolytic Flux and Acidosis Adaptation. The concurrent up-regulation of TPI1 and SLC16A1 (MCT1) highlights a synchronized mechanism designed to accelerate glycolysis and facilitate rapid lactate efflux, which supports biomass production and protects tumor cells from intracellular acidosis.
- The COA8 Metabolic Checkpoint. The specific down-regulation of COA8 in T2N1 and T3N2 stages acts as a precise molecular bottleneck that actively suppresses oxidative phosphorylation by disrupting Complex IV assembly, effectively forcing the bioenergetic reliance of NPC cells onto glycolysis.
- The lack of significance in T1N1. It does not weaken the model; rather, it underscores that the hybrid metabolic phenotype is a specialized hallmark of advanced, high-risk regional progression.

Competing interests

The authors declare no competing interest

Acknowledgements

This work has not been awarded grants by any Institution. The authors acknowledges NCBI GEO database contributors

Supplementary Material

Table 1S. Functional annotation of key genes associated with the Warburg effect hallmark in cancer metabolic reprogramming

References

1. Josephine Chou, Yu-Ching Lin, Jae Kim, Liang You, Zhidong Xu, Biao He, David M Jablons. Nasopharyngeal carcinoma--review of the molecular mechanisms of tumorigenesis. Head Neck 30(7):946-63. 2008. PMID: 18446839. doi: 10.1002/hed.20833.
2. Yu-Pei Chen, Anthony T C Chan, Quynh-Thu Le, Pierre Blanchard, Ying Sun, Jun Ma. Nasopharyngeal carcinoma. Lancet 394(10192):64-80. 2019. PMID: 31178151. doi: 10.1016/S0140-6736(19)30956-0.

3. Paul J Farrell. Epstein-Barr Virus and Cancer. Annu Rev Pathol 14:29-53. 2019. .PMID: 30125149. doi: 10.1146/annurev-pathmechdis-012418-013023.
4. Pok Man Hau, Hong Lok Lung, Man Wu, Chi Man Tsang, Ka-Leung Wong, Nai Ki Mak, Kwok Wai Lo. Targeting Epstein-Barr Virus in Nasopharyngeal Carcinoma. Front Oncol 10:600. 2020. PMID: 32528868. doi: 10.3389/fonc.2020.00600.
5. Lawrence S. Young, Alan B. Rickinson. Epstein-Barr virus: 40 years on. Nat Rev Cancer. 4(10):757-68. 2004. PMID: 15510157. doi: 10.1038/nrc1452.
6. Lawrence S. Young, Christopher W. Dawson. Epstein-Barr virus and nasopharyngeal carcinoma. Chin J Cancer 33(12):581-90. 2014. PMID: 25418193 doi: 10.5732/cjc.014.10197.
7. Lori E Dodd, Srikumar Sengupta, I-How Chen, Johan A. den Boon, Yu-Juen Cheng, William Westra, Michael A. Newton, Beth F. Mittl, Lisa McShane, Chien-Jen Chen, Paul Ahlquist, Allan Hildesheim. Genes involved in DNA repair and nitrosamine metabolism and those located on chromosome 14q32 are dysregulated in nasopharyngeal carcinoma. Cancer Epidemiol Biomarkers Prev 15(11):2216-25. 2006. PMID: 17119049 doi: 10.1158/1055-9965.EPI-06-0455.
8. Srikumar Sengupta, Johan A. den Boon, I-How Chen, Michael A. Newton, David B. Dahl, Meng Chen, Yu-Juen Cheng, William H Westra, Chien-Jen Chen, Allan Hildesheim, Bill Sugden, Paul Ahlquist. Genome-wide expression profiling reveals EBV-associated inhibition of MHC class I expression in nasopharyngeal carcinoma. Cancer Res 66(16):7999-8006. 2006. PMID: 16912175. doi: 10.1158/0008-5472.
9. Wan-Lun Hsu, Ka-Po Tse, Sharon Liang, Yin-Chu Chien, Wen-Hui Su, Kelly J Yu, Yu-Juen Cheng, Ngan-Ming Tsang, Mow-Ming Hsu, Kai-Ping Chang, I-How Chen, Tzu-I Chen, Czau-Siung Yang, Alisa M Goldstein, Chien-Jen Chen, Yu-Sun Chang, Allan Hildesheim. Evaluation of human leukocyte antigen-A (HLA-A), other non-HLA markers on chromosome 6p21 and risk of nasopharyngeal carcinoma. PLoS One 7(8):e42767. 2012. PMID: 22880099 doi: 10.1371/journal.pone.0042767
10. Natalya N Pavlova, Craig B Thompson. The Emerging Hallmarks of Cancer Metabolism. Cell Metab 23(1):27-47. 2016. PMID: 26771115. doi: 10.1016/j.cmet.2015.12.006.
11. Douglas Hanahan. Hallmarks of Cancer: New Dimensions. Cancer Discov 12(1):31-46. 2022. PMID: 35022204. doi: 10.1158/2159-8290.
12. Otto Warburg. On the origin of cancer cells. Science 123(3191):309-14. 1956. PMID: 13298683. doi: 10.1126/science.123.3191.309.
13. Coia Romeu, Maria-Jose Oliach, Antonio R. Romeu. Transcriptomic Profiling of Highly Expressed Genes Stratifies Nasopharyngeal Carcinoma Progression and Highlights Transferrin Receptor Dysregulation: A Bioinformatic Approach, 08 June 2026, PREPRINT (Version 1) available at Research Square [https://doi.org/10.21203/rs.3.rs-9935130/v1].
14.Maria-Jose Oliach, Coia Romeu, Antonio R. Romeu. Stage-Independent Downregulation of the GSTA1/GSTA3 Gene Cluster on Chromosome 6p12 as a Metabolic Hallmark of Nasopharyngeal Carcinoma, 22 June 2026, PREPRINT (Version 1) available at Research Square [https://doi.org/10.21203/rs.3.rs-10112864/v1].
15. Ron Edgar, Michael Domrachev, Alex E Lash. Gene Expression Omnibus: NCBI gene expression and hybridization array data repository. Nucleic Acids Res 30(1):207-10.2002. PMID: 11752295. doi: 10.1093/nar/30.1.207.
16. Tanya Barrett, Dennis B Troup, Stephen E Wilhite, Pierre Ledoux, Carlos Evangelista, Irene F Kim, Maxim Tomashevsky, Kimberly A Marshall, Katherine H Phillippy, Patti M Sherman, Rolf N Muertter, Michelle Holko, Oluwabukunmi Ayanbule, Andrey Yefanov, Alexandra Soboleva. NCBI GEO: archive for functional genomics data sets--10 years on. Nucleic Acids Res 39(Database issue):D1005-10.2011. PMID: 21097893. doi: 10.1093/nar/gkq1184.

17. Chin-Chih Lin, Tsung-Lin Cheng, Wen-Hui Tsai, Hui-Ju Tsai, Keng-Hsun Hu, Hao-Chun Chang, Chin-Wei Yeh, Ying-Chou Chen, Ching-Chun Liao, Wen-Tsan Chang. Loss of the respiratory enzyme citrate synthase directly links the Warburg effect to tumor malignanc. Sci Rep 2012:2:785. PMID: 23139858. doi: 10.1038/srep00785.
18. Shuang Liu, Tom Cadoux-Hudson, Christopher J Schofield. Isocitrate dehydrogenase variants in cancer — Cellular consequences and therapeutic opportunities. Curr Opin Chem Biol 57:122–134. 2020. PMID: 32777735. doi: 10.1016/j.cbpa.2020.06.012.
19. Justin Chak Ting Cheung, Lok Wan Ng, Zhongxu Zhu, Bonan Chen, Stephen Li, Mingjing Xu, Xiaofan Ding, Dandan Pu, Yi Hu, Yuqing Ren, Wei Kang, Ming Li, Jason Wing Hon Wong, Xin Wang, Yuen Kit Cheng, Wei Shen Aik, Ka Leung Wong, Simon Siu Man Ng, Nathalie Wong, Yujuan Dong. A Citrate Synthase Splice Variant Rewires the TCA Cycle to Promote Colorectal Cancer Progression. Cancer Res 85(22):4450-4468. 2025. PMID: 40900036. doi: 10.1158/0008-5472.CAN-24-2355.
20. Zhiduan Cai, Yulin Deng, Jianheng Ye, Yangjia Zhuo, Zezhen Liu, Yingke Liang, Hui Zhang, Xuejin Zhu, Yong Luo, Yuanfa Feng, Ren Liu, Guo Chen, Yongding Wu, Zhaodong Han, Yuxiang Liang, Funeng Jiang, Weide Zhong. Aberrant Expression of Citrate Synthase is Linked to Disease Progression and Clinical Outcome in Prostate Cancer. Cancer Manag 12:6149-6163. 2020. PMID: 32801864. doi: 10.2147/CMAR.S255817.
21. Lilan Chen, Ting Liu, Jinhua Zhou, Yunfei Wang, Xinran Wang, Wen Di, Shu Zhang. Citrate synthase expression affects tumor phenotype and drug resistance in human ovarian carcinoma. PLoS One 9(12):e115708. 2014. PMID: 25545012. doi: 10.1371/journal.pone.0115708. eCollection 2014.
22. Aiora Cenigaonandia-Campillo, Ana Garcia-Bautista, Anxo Rio-Vilariño, Arancha Cebrian, Laura Del Puerto, José Antonio Pellicer, José Antonio Gabaldón, Horacio Pérez-Sánchez, Miguel Carmena-Bargueño, Carolina Meroño, Javier Traba, María Jesús Fernandez-Aceñero, Natalia Baños-Herraiz, Lorena Mozas-Vivar, Estrella Núñez-Delicado, Jesús Garcia-Foncillas, Óscar Aguilera. Vitamin-C-dependent downregulation of the citrate metabolism pathway potentiates pancreatic ductal adenocarcinoma growth arrest. Mol Oncol 18(9):2212-2233. 2024. PMID: 38425123. doi: 10.1002/1878-0261.13616.
23. Lilan Chen, Ting Liu, Jinhua Zhou, Yunfei Wang, Xinran Wang, Wen Di, Shu Zhang. Citrate synthase expression affects tumor phenotype and drug resistance in human ovarian carcinoma. PLoS One. 9(12):e115708. 2014. PMID: 25545012. doi: 10.1371/journal.pone.0115708.
24. Liqing Guo, Zhi Wang, Yanpeng Fu, Shuhong Wu, Yaqiong Zhu, Jiasheng Yuan, Yuehui Liu. MiR-122-5p regulates erastin-induced ferroptosis via CS in nasopharyngeal carcinoma. Sci Rep 14(1):10019. 2024. PMID: 38693171. doi: 10.1038/s41598-024-59080-w.

Table 1. Differential Expression Statistics for the Six-Gene Metabolic Signature Across Advanced Clinical Stages in NPC

Clinical Stage	Gene Symbol	Probe ID	log2FC	Linear FC	AveExpr	t-statistic	P-Value	adj.P.Val	B-statistic
T2N1	LDHA	200650_s_at	0.9936	1.991	12.4196	3.9933	3.04E-04	0.0111	0.2831
	MRPL3	208787_at	0.9652	1.952	11.2621	4.1885	1.71E-04	0.0105	0.8077
	TIMMDC1	223004_s_at	0.9021	1.869	10.4496	4.2943	1.25E-04	0.0105	1.0954
	CYC	208905_at	0.9664	1.954	11.6977	4.1501	1.92E-04	0.0105	0.7040
	CS	208660_at	0.8720	1.830	10.8736	4.7920	2.79E-05	0.0092	2.4716
	GAPDH	AFFX-HUMGAPDH/ M33197_3_at	0.9000	1.866	13.0137	4.4134	8.76E-05	0.0105	1.4215
T2N2	LDHA	200650_s_at	1.1651	2.243	12.4196	4.4688	7.42E-05	0.0015	1.5280
	MRPL3	208787_at	1.1709	2.251	11.2621	4.8489	2.34E-05	0.0009	2.6108
	TIMMDC1	223004_s_at	1.0486	2.068	10.4496	4.7637	3.04E-05	0.0009	2.3666
	CYC	208905_at	1.2294	2.345	11.6977	5.0385	1.31E-05	0.0009	3.1570
	CS	208660_at	1.0067	2.009	10.8736	5.2796	6.24E-06	0.0007	3.8553
	GAPDH	AFFX-HUMGAPDH/ M33197_3_at	1.1398	2.203	13.0137	5.3339	5.28E-06	0.0007	4.0129
T3N2	LDHA	200650_s_at	1.0599	2.085	12.4196	4.5690	5.48E-05	0.0027	1.7895
	MRPL3	208787_at	1.1912	2.283	11.2621	5.5444	2.76E-06	0.0005	4.6198
	TIMMDC1	223004_s_at	1.2201	2.330	10.4496	6.2300	3.32E-07	0.0001	6.6282
	CYC	208905_at	0.9378	1.916	11.6977	4.3198	1.16E-04	0.0035	1.0838
	CS	208660_at	0.7946	1.735	10.8736	4.6832	3.88E-05	0.0027	2.1164
	GAPDH	AFFX-HUMGAPDH/ M33197_3_at	0.9404	1.919	13.0137	4.9461	1.74E-05	0.0019	2.8743

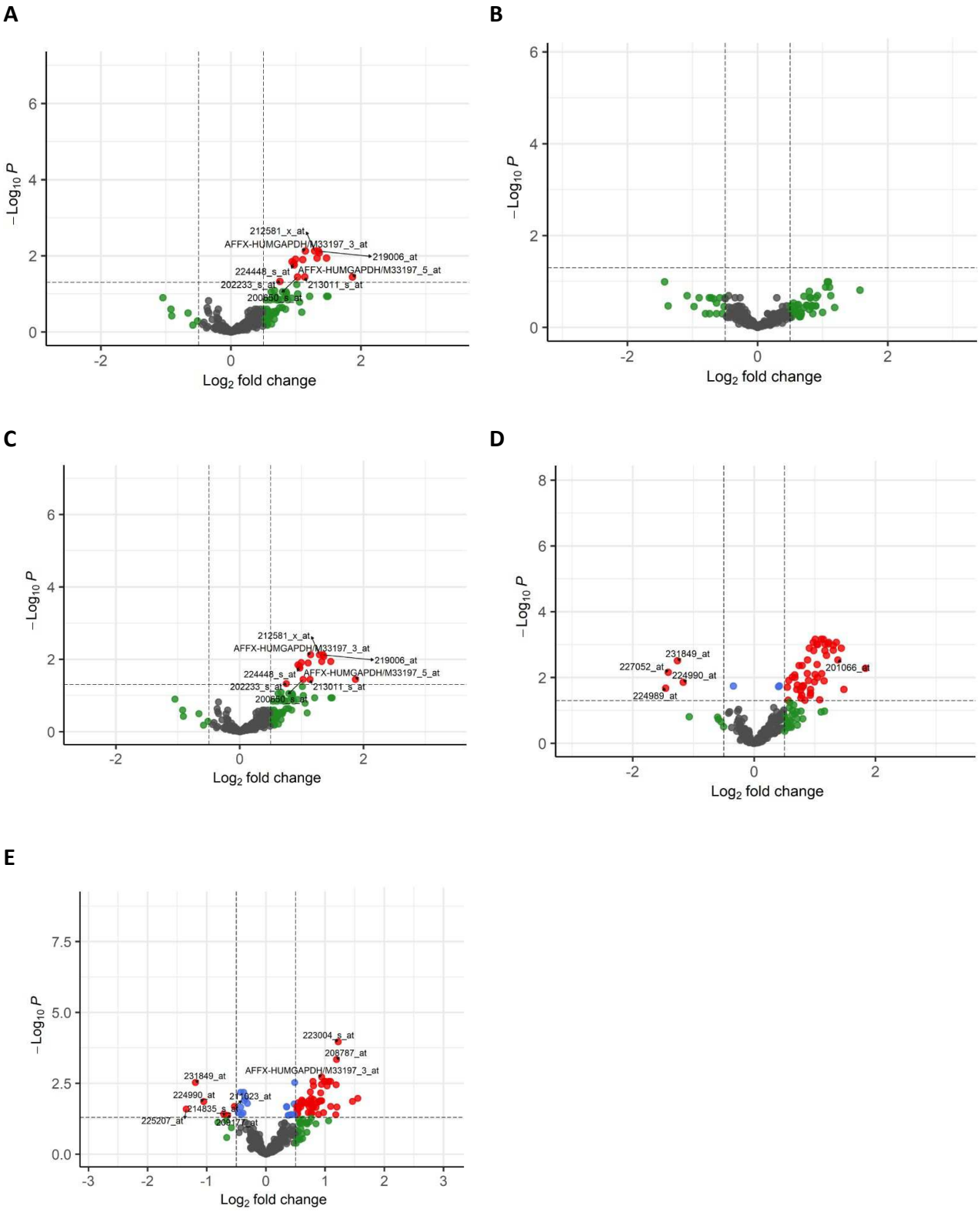
Data derived from NCBI GEO GDS3341 (GSE12452) dataset using the limma package in R. Log_2FC indicates log2 fold change relative to baseline controls. Linear FC represents the directional raw fold change. P-values were adjusted for multiple testing using the Benjamini-Hochberg False Discovery Rate (FDR) method (adj.P.Val). The B-statistic denotes the empirical Bayes log-odds of differential expression.

Table 2. Differential expression profile of Warburg effect-associated genes across nasopharyngeal carcinoma (NPC) developmental stages.

Symbol	GeneID	Gene_Title	Via_Metabolica	ProbeID	T1N0	T1N1	T2N1	T2N2	T3N2
TPI1	7167	triosephosphate isomerase 1	Glicolisis	200822_x_at					
GAPDH	2597	glyceraldehyde-3-phosphate dehydrogenase	Glicolisis	AFFX-HUMGAPDH/M33197_3_at					
CS	1431	citrate synthase	Ciclo_Krebs	208660_at					
SDHC	6391	succinate dehydrogenase complex subunit C	Cadena_Respiratoria	238191_at					
NDUFAF4	29078	NADH:ubiquitone oxidoreductase complex assembly factor 4	Cadena_Respiratoria	219006_at					
NDUFAF5	79133	NADH:ubiquitone oxidoreductase complex assembly factor 5	Cadena_Respiratoria	227160_s_at					
CYC	54205	cytochrome c, somatic	Cadena_Respiratoria	208905_at					
UQCRH	7388	ubiquinol-cytochrome c reductase hinge protein	Cadena_Respiratoria	202233_s_at					
TIMMDC1	51300	translocase of inner mitochondrial membrane domain	Cadena_Respiratoria	223004_s_at					
UQCC1	55245	ubiquinol-cytochrome c reductase complex chaperone 1	Cadena_Respiratoria	217935_s_at					
UQCC2	84300	ubiquinol-cytochrome c reductase complex chaperone 2	Cadena_Respiratoria	224448_s_at					
COA8	144501	cytochrome c oxidase assembly factor 8	Cadena_Respiratoria	231849_at					
TMEM70	54968	transmembrane protein 70	Cadena_Respiratoria	219448_at					
ATP12	23456	ATPAF2 ATP synthase mitochondrial F1 complex	Cadena_Respiratoria	223320_s_at					
TFAM	7019	transcription factor A, mitochondrial	Cadena_Respiratoria	203177_x_at					
MRPL3	11222	mitochondrial ribosomal protein L3	Cadena_Respiratoria	208787_at					
SLC16A1	6566	solute carrier family 16 member 1	Efecto_Warburg	209900_s_at					
LDHA	3939	lactate dehydrogenase A	Efecto_Warburg	200650_s_at					

Colors represent significant differential expression changes compared to early-stage or control baselines using the *limma* package (djusted *p*-value < 0.05; Log_2FC > 0.5). Red blocks indicate up-regulation, while green blocks indicate down-regulation. All listed genes are up-regulated across the specified stages, except for *COA8*, which is significantly down-regulated in the T2N1 and T3N2 stages. These genes are part of the 155 related genes in Table 1S with differential expression profile.

Figure 1. Volcano plots of differential metabolic gene expression across progressive clinical stages of nasopharyngeal carcinoma (NPC)



Differential expression analysis was performed on 155 functional annotation of key genes associated with the Warburg effect hallmark in cancer metabolic reprogramming (Table 1S) from the NCBI GEO GDS3341 / GSE12452 dataset using the limma package in R, comparing non-tumor control tissues against progressive tumor stages: (**A**) T1N0, (**B**) T1N1, (**C**) T2N1, (**D**) T2N2, and (**E**) T3N2. The plots illustrate the distribution of log_2 fold changes (x-axis) against the statistical significance $-log_{10}$ P-value (y-axis) for each clinical contrast.Horizontal and vertical dashed lines denote the statistical thresholds established for significance adjusted P-value< 0.05) via the Benjamini-Hochberg False Discovery Rate correction, and log_{2F}old Change(FC) > 0.5. Note the transition toward advanced clinical progression (C to E), where a highly selective subset of six genes (LDHA, GAPDH, CS, CYC, MRPL3, and TIMMDC1) emerges as consistently and robustly upregulated (top right quadrants) (Table 1), contrasting with the statistical stability maintained by the remaining metabolic and oxidative phosphorylation genes. Color coding of points: gray not significant; green significant by Log_2FC; red significant by P-value and Log_2FC.

Supplementary Files

This is a list of supplementary files associated with this preprint. Click to download.

- Table1S.xlsx